Article Type: Letter

Title: Higher methanotroph abundance and bottom-water methane in ponds with floating photovoltaic arrays

Running head: Floating solar and methane in ponds

Author Names: Nicholas E. Ray[1], Sophia Aredas[2], Steven M. Grodsky[3], Ash Canino[4], Simone J. Cardoso[5], Meredith A. Holgerson[6], Meredith Theus[6], Marian L. Schmidt[2]

Author Affiliations:
[1] School of Marine Science & Policy, University of Delaware, USA
[2] Department of Microbiology, Cornell University, USA
[3] U.S. Geological Survey, New York Cooperative Fish and Wildlife Research Unit, Department of Natural Resources and the Environment, Cornell University, USA
[4] Department of Natural Resources and Environment, Cornell University, USA
[5] Department of Zoology, Institute of Biological Sciences, Universidade Federal de Juiz de Fora, Brazil
[6] Department of Ecology and Evolutionary Biology, Cornell University, USA

Corresponding Author: Nicholas E. Ray; nickray@udel.edu

Author Contribution Statement:
NER designed the study, provided supplies, performed field sampling, laboratory analyses, and data analysis, and wrote the first draft of the manuscript. SA performed field sampling, laboratory analyses, data analysis, and edited the manuscript. SMG secured funding, constructed the floating solar arrays, performed field sampling, and edited the manuscript. AC, SJC, and MT performed field sampling and edited the manuscript. MAH secured funding, performed field sampling, and edited the manuscript. MLS designed the study, provided supplies, data analysis, secured funding, and edited the manuscript.

Scientific Significance Statement (125 word max)

Producing energy using floating photovoltaic (FPV) powerplants offers an opportunity to produce renewable energy, spare land, and reduce evaporation from ponds, lakes, and reservoirs. However, FPV deployment in these ecosystems is associated with colder temperatures, less oxygen availability, and changes in carbon cycling processes. Experimental evidence demonstrates an increase in concentrations of methane – a potent greenhouse gas – in ponds following FPV deployment. In this study, we investigate how microbial communities associated with aquatic methane cycling differ between ponds with and without FPV. We show that FPV deployment increases bottom-water methane concentrations and triggers dense blooms of methane-oxidizing bacteria that create a methane biofilter. These results provide the first evidence that microbial communities respond strongly to engineered shading and may help buffer greenhouse gas emissions in solar-covered waters.

Data and Code Availability

All raw and processed data for this project are publicly available. The code used for statistical comparisons, generating figures, and processing microbial community data are available on GitHub at https://github.com/MarschmiLab/Ray_LO_Letters_FPV_Methane. Biogeochemical data and summaries of methane cycling microbe abundances is available for download via the Figshare Repository (https://doi.org/10.6084/m9.figshare.29614025.v1). The raw, compressed 16S rRNA gene sequencing fastq files are available in the NCBI Sequence Read Archive (SRA) under the BioProject accession number PRJNA1417770 (https://www.ncbi.nlm.nih.gov/bioproject/1417770). All flow cytometry data are available for download from Zenodo (https://zenodo.org/records/18462017).

Abstract (150 words max)

Floating photovoltaic (FPV) arrays alter the methane (CH_4) cycling dynamics of waterbodies on which they are deployed. Here, we investigated dissolved CH_4 dynamics and associated CH_4 cycling microbial communities (methanogens and methanotrophs) in the second year of FPV deployment (70% aerial coverage) in experimental ponds. We found that bottom-water CH_4 concentrations were twice as high in ponds with FPV compared to those without, while surface water CH_4 concentrations were orders of magnitude lower than bottom-waters, but did not differ between treatments. There was no change in the relative abundances of putative sediment methanogens or methanotrophs, but FPV restructured methanogen communities. FPV promoted late-summer methanotroph blooms in the water column, with abundances surpassing 1,000,000 cells mL^{-1}. We conclude that prolonged periods of CH_4 production in low oxygen FPV ponds favored blooms of methanotrophs, that may mitigate diffusive CH_4 emissions to the atmosphere by consuming dissolved CH_4.

Keywords: pond, methane, floating solar, greenhouse gas, methanogen, methanotroph

Introduction

Methane (CH_4) emissions from aquatic ecosystems have increased because of human activity (Jackson et al. 2024). Floating photovoltaic arrays (FPV), first deployed in 2007, are a rapidly expanding renewable energy technology shown to alter aquatic CH_4 dynamics and emissions (Cazzaniga and Rosa-Clot 2021; Ray et al. 2024). By 2023, over 643 FPV power plants had been installed on lakes, ponds, and reservoirs worldwide (Nobre et al. 2024; Ramanan et al. 2024). There is substantial interest and potential in expanding FPV use on reservoirs and lakes to meet demands for renewable energy (Jin et al. 2023; Woolway et al. 2024), but the ecological and biogeochemical tradeoffs – particularly effects on CH_4 cycling – must be evaluated before broader deployment (Almeida et al. 2022; Gallaher et al. 2025).

FPV deployment is associated with lower water temperatures (Dörenkämper et al. 2021; Andini et al. 2022), reduced oxygen availability (Wang et al. 2022; Ray et al. 2024), and changes in stratification (Ilgen et al. 2023). These factors influence CH_4 dynamics in small, shallow systems where FPV has most commonly been deployed (Bastviken et al. 2004; Aben et al. 2017; Ray and Holgerson 2023; Nobre et al. 2024). Indeed, in the first year of FPV deployment, experimental ponds with FPV showed twice the dissolved CH_4 concentrations and CH_4 ebullition compared to control ponds without FPV, but diffusive CH_4 emissions were lower (Ray et al. 2024).

Determining how FPV affects methanogens (CH_4 producers) and methanotrophs (CH_4 consumers) is essential for understanding CH_4 dynamics in ecosystems with FPV. Methanogenic archaea and methanotrophic archaea and bacteria jointly regulate CH_4 dynamics, yet it remains unresolved how FPV-induced changes in temperature, light, oxygen, and primary production

influences their abundance, composition, and activity. Evidence from non-FPV settings suggests changes in these limnological conditions can re-structure CH4-cycling communities and alter metabolic rates (Wang et al. 2021; Bertolet et al. 2022). Clarifying microbial responses to FPV is critical for determining whether this technology amplifies or dampens CH_4 emissions and, more broadly, for understanding how pond microbial communities respond to reduced temperature, oxygen, and light.

Here, we investigate how FPV affects CH_4 dynamics in temperate experimental ponds during the second year of FPV deployment, with a focus on identifying microbial and biogeochemical mechanisms underlying dissolved CH_4 concentrations. We pair observations of temperature, dissolved oxygen, and dissolved CH_4 with measurements of methanogen and methanotroph community structure and CH_4 process rates during an intensive mid-summer sampling campaign in ponds with and without FPV. To capture microbial mechanisms relevant to dissolve CH_4 concentrations, we focus on well-characterized methanotrophs and integrate community data with functional rate measurements to capture both composition and activity.

Methods

Location and Sampling Scheme

In 2023, FPV arrays (70% aerial coverage) were deployed on three ponds at the Cornell Experimental Ponds Facility in Ithaca, New York, USA (42.5049 N, 76.4666 W). Observational sampling of six ponds starting in 2022 prior to FPV deployment in 2023, providing three replicate control and three replicate FPV ponds (Ray et al. 2024). Each pond is a 30 x 30 m

inverted, truncated pyramid, 1.75 m deep, unlined, and with sediment accumulation since construction in 1958-1959. Rooted, submerged macrophytes dominate primary production.

We returned in summer 2024 to continue measurements of dissolved CH_4 (surface and bottom), temperature, and dissolved oxygen (4 depths; 0.1, 0.75, 1, and 1.25 m from the water surface). We sampled methanogens and methanotrophs four times in 2024 from surface water, bottom water, and sediments. On July 11, 2024, we measured diffusive CH_4 exchange and net CH_4 production or consumption in surface waters, bottom waters, and sediments using bottle incubations (*Supplemental Methods*). For each date, we calculated density gradients of pond water columns using temperature profile data to compare mixing and stratification dynamics between ponds with and without FPV (*Supplemental Methods*).

Observational CH_4 Concentration Measurements

We collected samples to determine dissolved CH_4 concentrations in the surface and bottom water of each pond six times between June 20 and September 5. Samples were collected in triplicate from the pond center using a headspace equilibration approach, with surface samples collected by hand at 10 cm depth and bottom water collected using a Van-Dorn bottle ~10 cm from the sediment-water interface (Ray et al. 2024). Samples were stored in 12 mL pre-evacuated borosilicate exetainer vials until analysis using a gas chromatograph equipped with a flame ionization detector (Shimadzu GC-2014).

Microbial Sample Collection, Preservation, and Analysis

Water samples for microbial analysis were collected as for CH_4 measurements and sequentially filtered through 200 µm and 20 µm NYTEX mesh into 2 L Nalgene bottles and kept on ice until return to the lab the same day. Surface sediments (top 2 cm) were collected using a PVC pole corer and stored in WhirlPak bags in the cooler. Water was filtered onto 0.22 µm polyethersulfone filters using a peristaltic pump (190-2020 mL per sample). Sediments were homogenized using a stainless-steel coffee grinder (three 1 second pulses per sample). Filters (halved) and homogenized sediment were stored in 2 mL cryovials at -80 °C for until microbial DNA extraction, sequencing, and bioinformatics (*Supplemental Methods*). Samples for flow cytometry were fixed with 1 µL 25% glutaraldehyde, diluted 15–20×, stained with SYBR Green I, and run in triplicate on an Attune NxT (*Supplemental Methods*)

Diffusive CH_4 Flux Measurements and Estimation of k600

We measured diffusive fluxes at the center and edge of each pond using floating chambers (18.93 L volume; 0.071 m^2 cross sectional area) attached to a portable analyzer that determines CH_4 concentrations in air using off-axis integrated cavity output spectroscopy (GLA132-GGA, ABB Measurement and Analytics; Ray et al. 2024). At the same time, we collected headspace samples for determination of dissolved CH_4 concentrations. Using diffusive CH_4 flux measurements and dissolved CH_4 concentrations, we calculated gas transfer velocities (i.e., k_{600} values as:

$$k_{600} = \frac{CH_4\ Flux}{[CH_4]_{water} - [CH_4]_{equilibrium}} \times \left(\frac{600}{S_c}\right)^{-n}$$

Where S_c and n are the Schmidt number for CH_4 and the Schmidt number exponent, respectively.

91

92 **Statistical Comparisons**

93 All statistical analyses were performed using R statistical software and figures were made using
94 the *ggplot2* package (Wickham 2016). We considered the results of statistical tests to be
95 significant when $p < 0.05$.

96

97 We fit linear mixed-effects models (fixed: treatment, day of year; random: pond) to compare
98 environmental and microbial metrics in ponds with FPV compared to those without FPV (i.e.,
99 control) ponds using *lme4* (Bates et al. 2015; Table S2). Rates of water column CH_4 production
100 or consumption in surface and bottom waters were compared using a mixed effects model of
101 light or dark bottle and FPV presence with pond as a random effect (Table S3). Contrasts
102 between treatments were made using least square means tests via *emmeans* (Lenth 2018) (Table
103 S4).

104

105 Water temperature and oxygen were depth-averaged by pond and day. Diffusive CH_4 fluxes,
106 k600, and potential sediment CH_4 production were compared using two-tailed t-tests (Tables
107 S5&6).

108

109 Bray–Curtis dissimilarities were visualized with principal coordinates analysis (PCoA) and
110 tested using PERMANOVA (adonis2), β-dispersion (betadisper), Mantel tests, and Procrustes
111 analysis in *vegan* (Oksanen et al. 2018). Water column ASVs were analyzed as absolute
112 abundances by scaling relative sequence abundances to total microbial cell counts (cells mL^{-1}),
113 whereas sediment ASVs were analyzed as relative abundances following rarefaction.

Differentially abundant ASVs were identified with ANCOMBC-II (prevalence ≥5%), testing for a time-averaged FPV effect without temporal interactions and retaining ASVs with a FDR-adjusted $q < 0.05$ and $|\log_2 \text{ fold change}| > 0.5$ (Lin and Peddada 2024). To complement these tests, we additionally applied a seasonally explicit, time-resolved ASV-level screening to visualize FPV treatment separation at individual sampling dates (Supplemental Methods)

Results

FPV Ponds had Higher CH_4 Concentrations at Depth

Dissolved CH_4 concentrations were relatively stable over time (Fig. 1A & 1C). Surface CH_4 did not differ between ponds with FPV (1.79 ± 4.01 µmol CH_4 L^{-1}) and control ponds without FPV (2.07 ± 3.19 µmol CH_4 L^{-1}; $p = 0.208$; Fig. 1B). However, bottom water CH_4 was two orders of magnitude higher than in surface waters, and more than twice as high in ponds with (306.2 ± 419.0 µmol CH_4 L^{-1}) than control ponds (129.7 ± 45.60 µmol CH_4 L^{-1}; $p = 0.003$; Fig. 1D).

FPV Ponds were Colder and Less Oxygenated

Ponds with FPV were almost 4 °C colder across the water column (18.87 ± 1.69 °C; mean ± SD) than control ponds (22.78 ± 2.29 °C) during summer ($p < 0.001$; Fig. S1). On average, ponds could be considered stratified (i.e., density gradient > 0.29 kg m^{-3} m^{-1}; Holgerson et al 2022), but we found no evidence that FPV changed pond mixing and stratification patterns, as mean density gradients in FPV ponds (0.76 ± 0.63 kg m^{-3} m^{-1}) were similar to control ponds (0.62 ± 0.42 kg m^{-3} m^{-1}; $p = 0.180$). While all ponds were generally undersaturated in DO, surface waters in control ponds were occasionally oversaturated, unlike FPV ponds, which remained undersaturated

throughout the sampling period (Fig. S2; Table S7). Mean DO in FPV ponds (2.70 ± 0.98 mg L^{1}) was half that of control ponds (5.42 ± 2.20 mg L^{-1}; $p < 0.001$; Fig. 1 E-H & Fig. S3).

FPV Ponds had Higher Water Column Methanotroph Abundance

Water column methanotroph abundance showed increasing divergence between ponds with and without FPV as the season progressed. In surface waters, methanotroph abundance was 3.7 times higher in FPV ponds (4.4 ± 3.7 x 10^5 cells mL^{-1}) than ponds without FPV on average (1.2 ± 1.0 x 10^5 cells mL^{-1}; $p = 0.021$; Fig. 2A-B). Bottom waters displayed similar trends, with 2.8. times more methanotrophs in FPV ponds (Fig. 2E-H). Abundance of methanogens in the water column was orders of magnitude lower than methanotrophs and there were no differences between treatments (Fig. 2C & D). Methanogens averaged ~20% of the sediment community and were more abundant than methanotrophs (~6%), but neither group differed between treatments (Fig. 2I-L).

Methanotroph Blooms and Seasonal Functional Redundancy in Sediment Methanogens in FPV Ponds

FPV altered methanotroph and methanogen community composition in both water and sediments (Fig. 4 & S4; Table S8 & S9), producing stronger group separation than pond identity across all comparisons (Table S8 & S9). Community composition varied with day of year (DOY), with significant FPV x DOY and pond x DOY interactions in both habitats. Spatial structuring by FPV presence and pond identity was more pronounced in sediments than in the water column. Water column community structure was tightly coupled with methanotroph composition rather than methanogens, indicated by strong correlations between water column community structure

159 and methanotroph composition, supported by Mantel ($r = 0.996$, $p < 0.001$) and Procrustes
160 (correlation = 0.999, m12 = 0.002, $p < 0.001$) analyses. At the class level, FPV restructuring of
161 water-column methanotrophs was driven by increased gammaproteobacterial (Type I) abundance
162 under FPV and higher alphaproteobacterial (Type II) abundance in ponds without FPV, whereas
163 sediment methanotroph classes showed limited treatment separation and FPV-associated effects
164 were most evident in Methanosarcinia (Fig. S4).
165
166 FPV altered seasonal trajectories in sediment methanogen communities, but not methanotroph
167 communities (Table S9). For both methanogens and methanotrophs, community composition
168 was structured primarily by pond identity, with additional contributions from FPV and DOY, and
169 for methanogens, a significant FPV x DOY interaction indicating FPV-specific seasonal shifts
170 (Fig. S5A & B; Table S9).
171
172 FPV-associated shifts in water column methanotrophs were driven by a small number of Type 1
173 (hereafter gammaproteobacterial) methanotrophic ASVs in the family Methylomonadaceae (Fig.
174 4). Four gammaproteobacterial methanotrophic ASVs within the order Methylococcales were 3-
175 12x enriched in FPV ponds compared to controls. The strongest enrichment was observed for
176 ASV_32 (*Methyloparacoccus*, family Methylococcaceae), which increased almost 12x under
177 FPV. Additional enriched ASVs belonged to the family Methylomonadaceae, including
178 ASV_141 (*Methylobacter_C*), ASV_13 (genus unresolved), and ASV_119 and ASV_44
179 (*Methylomonas alba*), which each increased ~3-4x (Fig. 4A). Collectively, these taxa reached
180 abundances exceeding 300,000 cells mL^{-1} in FPV ponds. Six gammaproteobacterial
181 methanotroph ASVs within the family Methylococcaceae declined under FPV (~3x lower

abundance), including multiple ASVs classified as *Methyloterricola oryzae* (Fig. 4B). These taxa occurred at much lower abundances and were more abundant in the bottom water (Fig. 4), remaining one to two orders of magnitude less abundant than FPV enriched methanotrophs (Fig. 4). Unlike methanotrophs, water-column methanogen ASVs were sparse but three ASVs had modest enrichment in ponds without FPV (Fig. S6).

In sediments, time-averaged analyses detected several ASVs enriched in ponds without FPV, while few were enriched in FPV ponds (Fig. S7). However, sediment methanogen communities exhibited a significant FPV x DOY interaction (Table S9), indicating seasonal dynamics not captured by time-averaged analyses. Accordingly, a seasonally explicit (time-resolved) approach revealed FPV-associated divergent trajectories spanning hydrogenotrophic, acetoclastic, and methylotrophic methanogens, indicating cross-genus functional redundancy in FPV responses across 18 ASVs (Fig. 5). In contrast, seasonally explicit FPV responses among sediment methanotrophs were limited to only eight ASVs spanning multiple methanotrophic types (Fig. S8), consistent with more limited functional redundancy in methane oxidation. Time-averaged patterns were dominated by functionally diverse ASVs enriched in ponds without FPV, whereas enrichment in ponds with FPV was limited to a small, constrained set of hydrogenotrophic methanogens and a single anaerobic methanotroph (Fig. S7).

No Apparent Differences in CH_4 Cycling Processes

We found no differences in diffusive water-air CH_4 exchange or gas transfer velocities between ponds with and without FPV or between the center and edge of ponds (Table S5&10). On average, all ponds emitted CH_4 to the atmosphere at a rate of 404.1 ± 896.6 μmol CH_4 m^{-2} h^{-1}.

We also found no difference in rates of water column CH_4 net-production or consumption between ponds with and without FPV (Table S3). Sediments from both ponds with and without FPV produced CH_4, but we found no difference in potential CH_4 production rates by sediments in ponds with FPV (5.43 ± 4.81 ppm CH_4 g dry sediment^{-1} d^{-1}) compared to those without (14.13 ± 10.92 ppm CH_4 g dry sediment^{-1} d^{-1}; $p = 0.303$; Table S6).

Discussion

Following FPV deployment, bottom waters sustained elevated dissolved CH_4 concentrations for a second year along with enhanced water column methanotroph abundances (Fig. 1D; Fig. 2) Surface water CH_4 – and diffusive CH_4 emissions – were similar between ponds with and without FPV. Together, these patterns suggest FPV-induced changes in redox conditions promote CH_4 accumulation in bottom-waters, while microbially mediated CH_4 oxidation dynamically constrains diffusive CH_4 fluxes to the atmosphere, positioning water column methanotrophs as a potentially critical biofilter.

Specifically, we hypothesize that prolonged low-oxygen conditions in FPV ponds facilitate longer periods of CH_4 accumulation in bottom waters overlying sediments. In response to this accumulation, water column methanotrophs reached bloom-like densities in late summer, exceeding 1,000,000 cells mL^{-1} and reaching abundances higher in ponds with FPV than those without (Fig 2A). The coexistence of a persistently large CH_4 pool and low, but not inhibitory, oxygen concentrations created conditions that selectively favored gammaproteobacterial methanotrophs later in the season, supporting elevated CH_4 oxidation throughout the water

227 column. By oxidizing CH_4, methanotrophs serve as a fundamental biological sink that likely
228 buffers diffusive CH_4 emissions.
229
230 Beyond CH_4 availability, FPV-driven hypoxia restructured microbial composition in a lineage-
231 and time-dependent manner. At the ASV level, closely related gammaproteobacterial
232 methanotrophs within the order *Methylococcales* exhibited divergent, family-level responses to
233 FPV across the season, with *Methylomonadaceae* ASVs strongly enriched and
234 *Methylococcaceae* ASVs declining in FPV conditions (Fig 4 & S5). Although both families
235 represent gammaproteobacterial (Type I) methanotrophs, *Methylomonadaceae* taxa like
236 *Methylomonas alba* demonstrate a "rapid response capability," with the potential to increase
237 abundance by two orders of magnitude in days under oxygen limited conditions (van Grinsven et
238 al., 2020). This physiological capacity is consistent with use of the ribulose monophosphate
239 (RuMP) pathway for carbon assimilation, which is more energy efficient than the serine pathway
240 used by alphaproteobacterial (Type II) methanotrophs and supports rapid growth under high CH_4
241 availability (Knief, 2015). The resulting dominance is further supported by metabolic flexibility,
242 including the genomic potential for fermentation and denitrification, which likely facilitates their
243 enigmatic persistence in anoxic zones (Reis et al., 2024). Conversely, *Methylococcaceae* like
244 *Methyloterricola oryzae* appear less responsive to transient hypoxia, as they are often found in
245 stable, well oxygenated surface waters (Reis et al. 2020). Thus, FPV does not uniformly enhance
246 gammaproteobacterial methanotrophs, but instead selectively favors specific
247 *Methylomonadaceae* lineages with life-history traits suited to rapidly exploiting FPV-induced
248 redox shifts.
249

250 A similar FPV x DOY signal emerged within sediment methanogen communities. Although
251 relative abundance did not differ by FPV presence (Fig 2K-L), a pattern commonly observed in
252 temperate lake sediments (Bertolet et al., 2019; Lyautey et al., 2021), ASV-level time series
253 revealed clear, treatment-specific seasonal trajectories across many of the most abundant
254 methanogens (Fig 5). These shifts in peak timing and magnitude likely reflect the response of
255 specific ASVs to changes in the supply of methanogenic precursors, such as acetate or hydrogen,
256 produced by syntrophic bacteria during the decomposition of settling organic matter (Bertolet et
257 al., 2019, 2022). This compositional divergence suggests a high degree of cross-genus functional
258 redundancy, with 18 methanogen ASVs spanning all three metabolic pathways responding to
259 FPV (Fig. 5). Such redundancy implies that methanogenesis is robust to FPV-induced
260 perturbation of community composition as many lineages can exploit a fluctuating pool of
261 metabolic byproducts (Rissanen et al., 2021). In contrast, sediment methanotroph responses were
262 more constrained (8 ASVs; Fig. S8), indicating lower functional redundancy (Reis et al., 2019,
263 2024). This divergence suggests that FPVs act as a deterministic environmental filter that
264 restructures the timing and internal organization of sediment methane cycling without altering
265 overall abundances (Fig. 2).
266
267 In late summer, methanotrophs surpassed 1,000,000 cells mL^{-1} in FPV surface and bottom
268 waters, a density rarely reported in any aquatic systems where previous concentrations peak
269 within 100,000 cells mL^{-1} (Milucka et al., 2015; Reis et al., 2019). These extreme bloom
270 magnitudes far exceed variation expected from differences in 16S rRNA operon copy number,
271 indicating true population-level expansion rather than methodological inflation, even relative to
272 CARD-FISH–based estimates. Blooms may result from the metabolic advantage of

gammaproteobacterial methanotrophs under CH_4 -rich, low-O_2 conditions, as observed in freshwater lakes where gammaproteobacterial methanotrophs proliferate under hypoxia and anoxia (Reis et al. 2020; Reis et al. 2024). Even under apparently anoxic conditions, aerobic methanotrophy may be sustained by cryptic O_2 cycling, in which oxygen produced by photosynthetic algae or cyanobacteria is rapidly consumed by methanotrophs (Milucka et al., 2015). Although light availability was not measured, shading from FPVs may further enhance methanotrophic dominance by suppressing photoinhibition or reducing phytoplankton competition (Murase & Sugimoto 2005; Thottathil et al. 2018).

Our results also demonstrate that the effect of FPV on pond biogeochemistry and CH_4 cycling varies over time. Immediately following FPV deployment in 2023, FPV ponds had lower oxygen concentrations and increased surface and bottom water CH_4 concentrations (Ray et al. 2024). By contrast, in the second year (2024), surface CH_4 concentrations no longer differed between treatments, and methanotroph abundance was substantially higher in FPV surface waters. These patterns suggest a time-lagged ecological response, where sustained hypoxia promotes bottom-water CH_4 accumulation, followed by methanotroph enrichment that buffers CH_4 flux near the surface. Quantifying how CH_4 ebullition responds to FPV deployment across seasons and years remains a key open question for understanding total emission dynamics.

Identifying strategies for low emission energy production is critical for combating climate change. As FPV expansion accelerates, understanding how this technology interacts with aquatic CH_4 dynamics is important for ensuring sustainability. Our study provides mechanistic evidence that FPV deployment can restructure microbial communities in ways that influence carbon

cycling, offering a foundation for evaluating the long-term ecosystem-level impacts of continued FPV proliferation across aquatic systems.

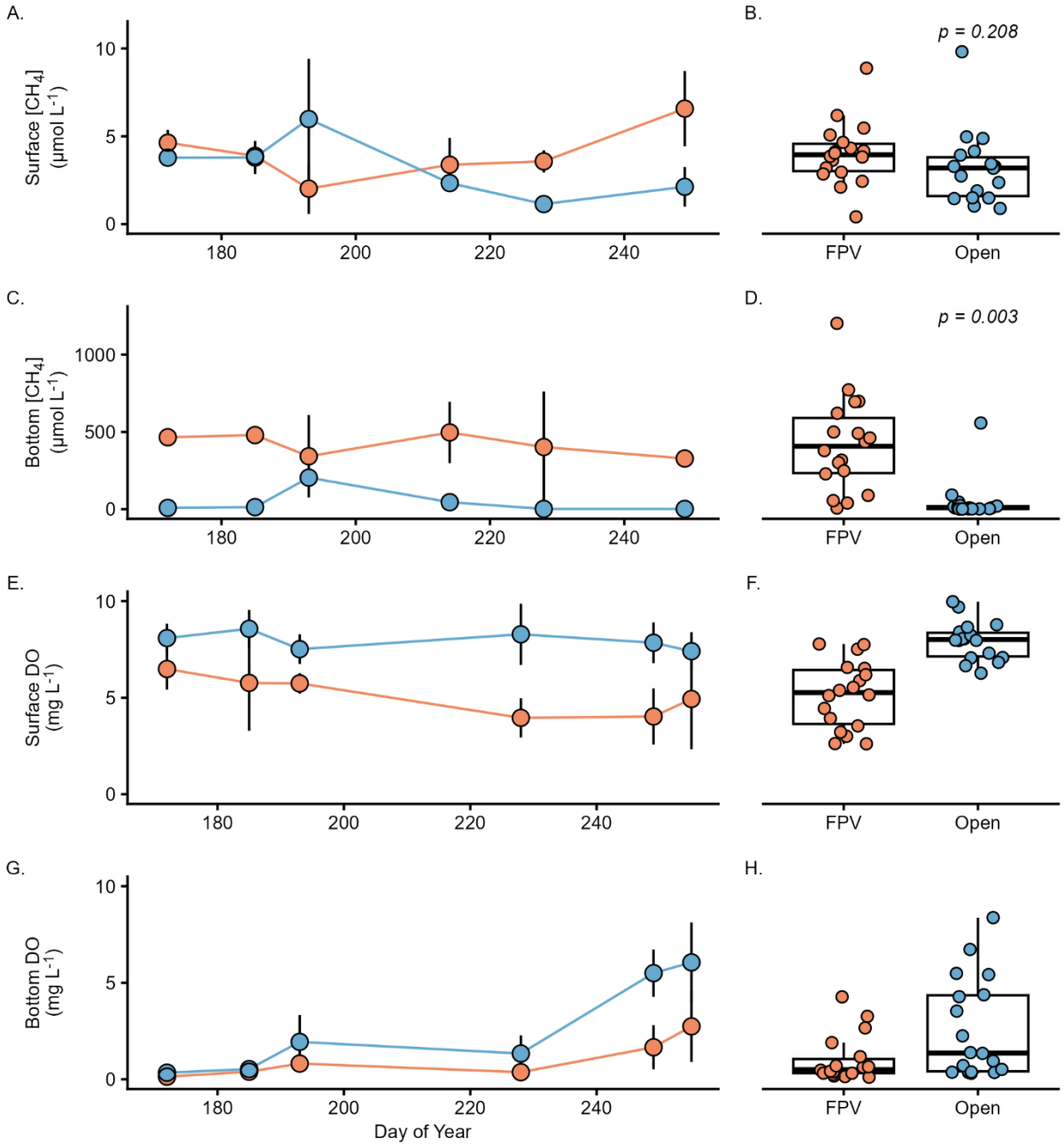

Fig. 1: Dissolved methane concentrations (A-D) and dissolved oxygen concentrations (E-H) in the surface (A, B, E, F) and bottom water (C, D, G, H) of ponds with and without floating photovoltaic (FPV) arrays in summer 2024. In (A, C, E, G) points indicate the mean CH_4 concentration from pond centers on a given date by treatment group and error bars indicate standard deviation. Colored lines connect the means. In panels (B, D, F, H) each point on the boxplot indicates a measured CH_4 concentration in an individual pond based on whether FPV is present (FPV) or not (Open) and p-values indicate the result of a least-squares mean test of the treatment effect of the mixed model (Table S3).

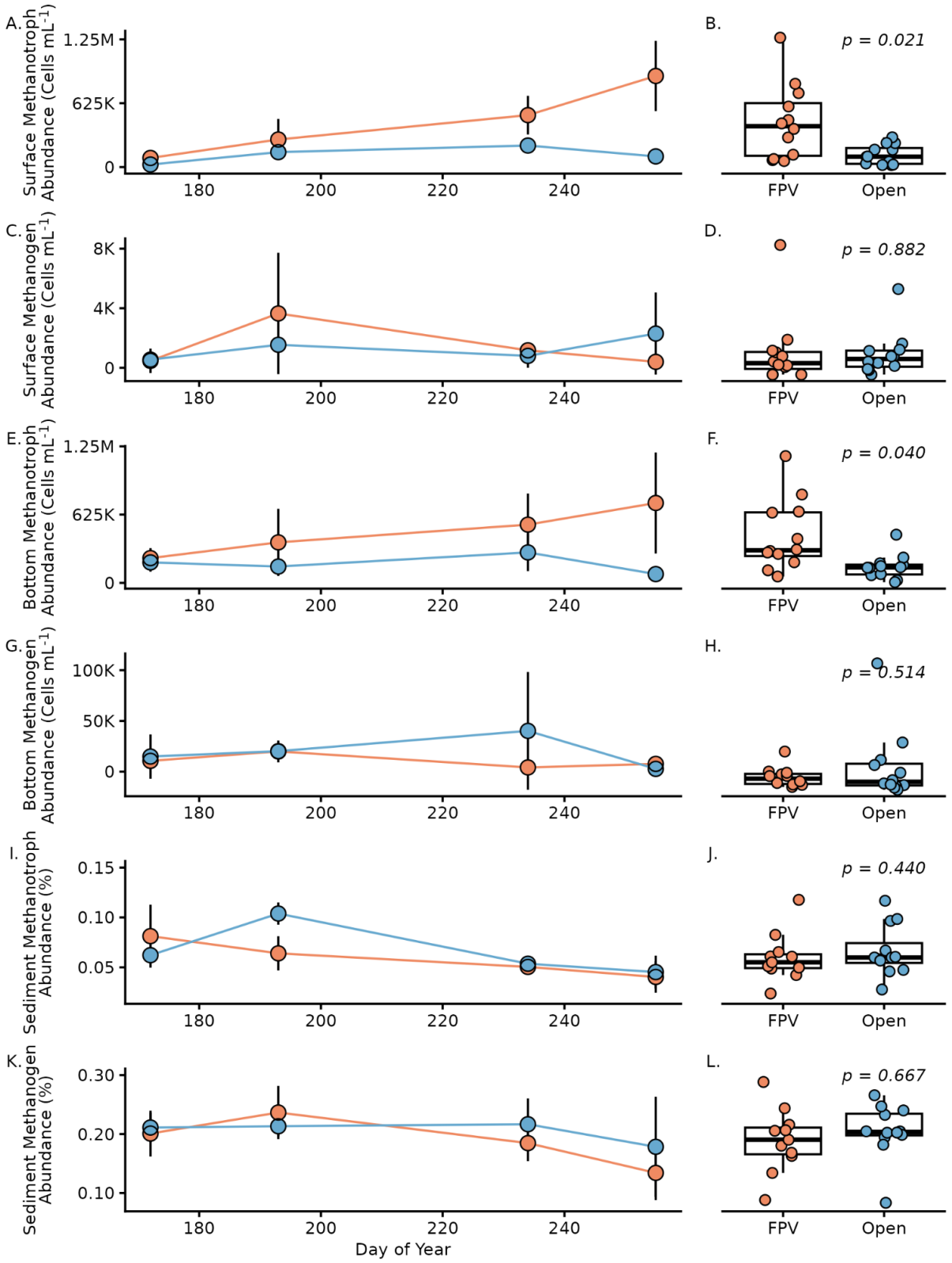
A.
Surface Methanotroph Abundance (Cells mL-1)
1.25M
625K
0
180
200
220
240
B.
p = 0.021
FPV
Open
C.
Surface Methanogen Abundance (Cells mL-1)
8K
4K
0
D.
p = 0.882
E.
Bottom Methanotroph Abundance (Cells mL-1)
F.
p = 0.040
G.
Bottom Methanogen Abundance (Cells mL-1)
100K
50K
H.
p = 0.514
I.
Sediment Methanotroph Abundance (%)
0.15
0.10
0.05
J.
p = 0.440
K.
Sediment Methanogen Abundance (%)
0.30
0.20
0.10
L.
p = 0.667
Day of Year

Fig. 2: Total abundance (A-H) of methanotrophs and methanogens in surface waters and bottom waters and relative abundance (I-L) of methanotrophs and methanogens in sediments of ponds with FPV ("FPV") and those without ("Open") in summer 2024. Information as for Fig. 1. P-values reflect least-square means test result of the mixed model (Table S3).

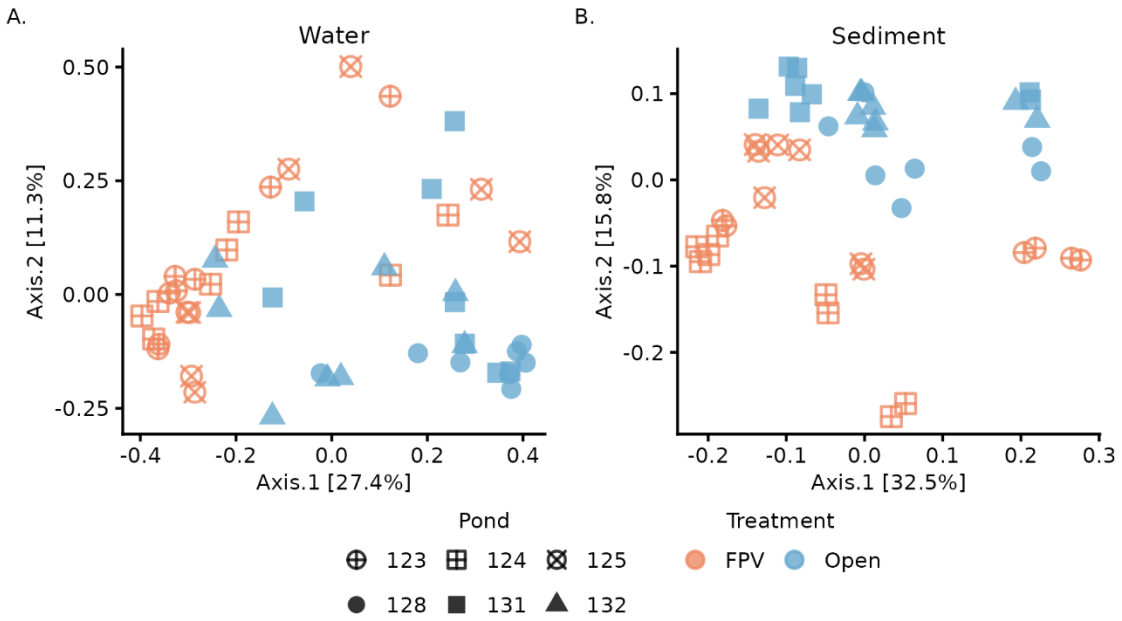

Fig. 3: Bray–Curtis PCoA of combined methanogen and methanotroph communities in ponds with FPV ("FPV") and ponds without FPV ("Open"). (A) Dissimilarity among water column samples was calculated using absolute cell abundances. (B) Sediment samples were rarefied to 20,826 reads to calculate dissimilarity based on relative abundance; replicates are shown separately. Shapes denote ponds.

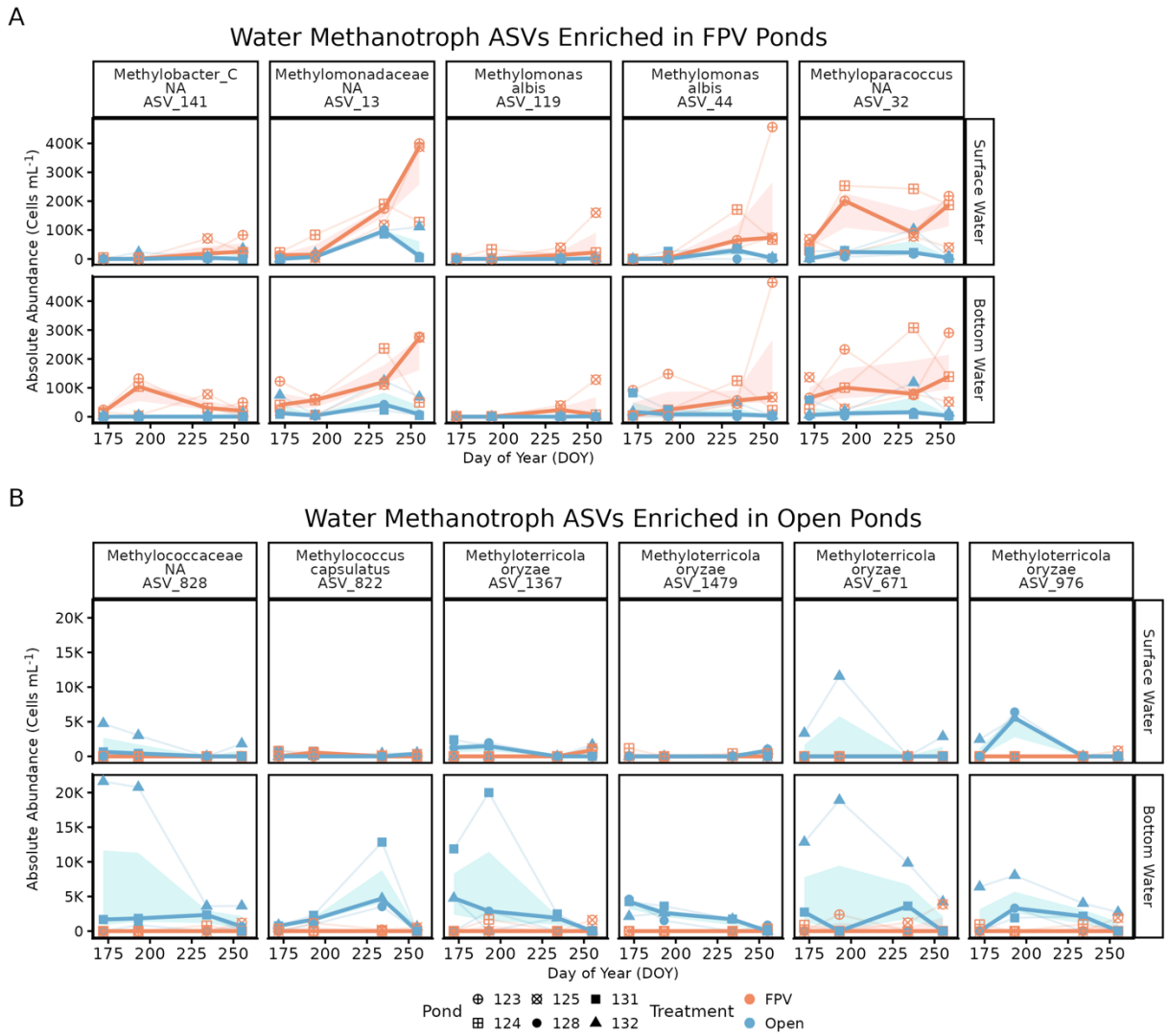

Fig. 4: Methanotroph ASVs identified as differentially abundant using time-averaged ANCOM-BC2 analyses are shown as absolute abundance (cells mL^{-1}) across the sampling season for ponds with FPV ("FPV") and ponds without FPV ("Open"). (A) ASVs exhibiting bloom-like increases under FPV infrastructure and (B) ASVs enriched in ponds without FPV installed. Taxonomic assignments are shown at the lowest resolved rank. For clarity, two low-abundance ASVs enriched in ponds with FPV (ASV_2028, ASV_346) and one ASV in ponds without FPV with minimal separation (ASV_1019) were omitted.

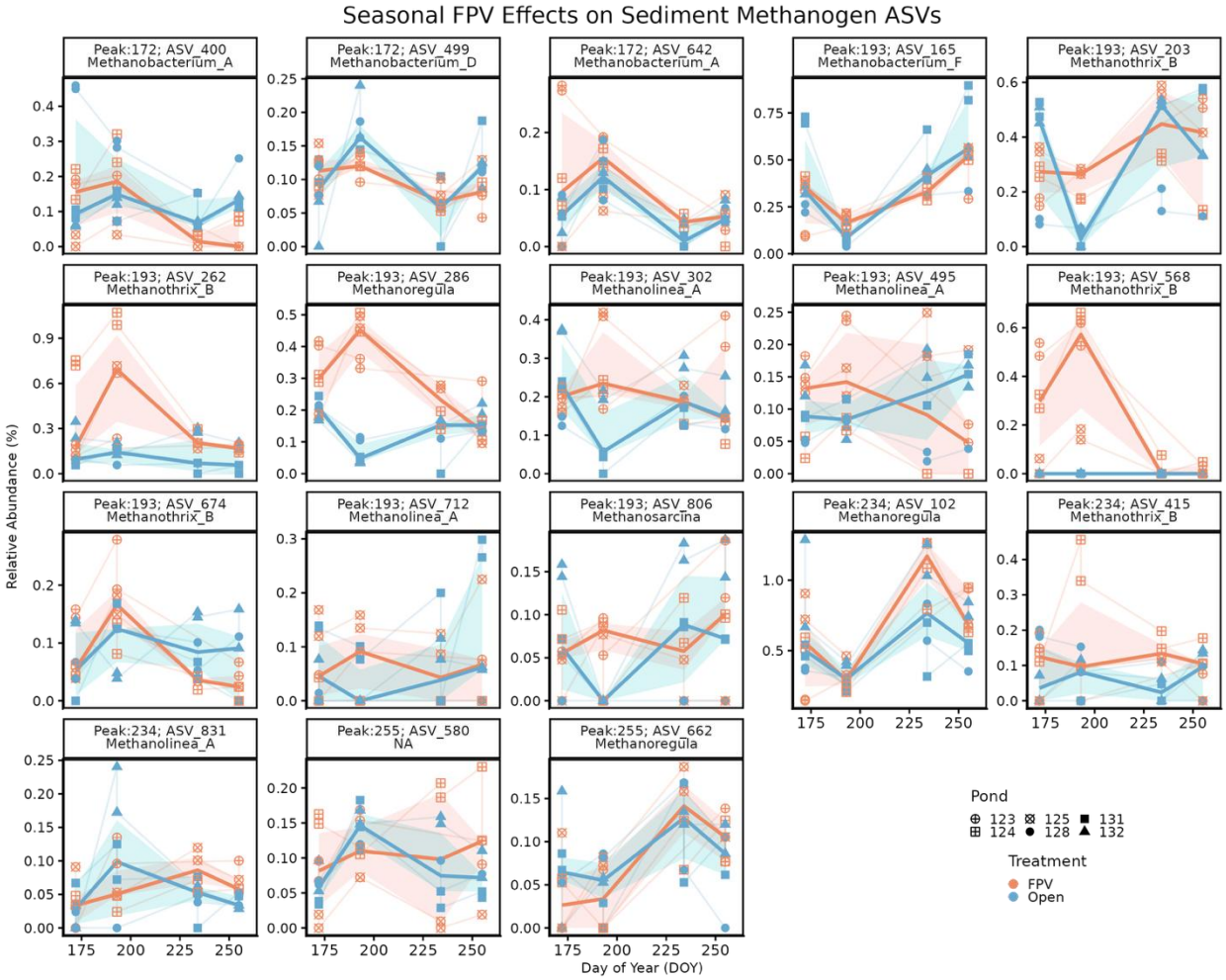

Fig. 5: Relative abundance (%) of sediment methanogen ASVs over time in ponds with FPV ("FPV") and ponds without FPV ("Open"). ASVs were identified using a seasonally explicit (time-resolved) screening approach targeting abundant taxa (mean relative abundance > 0.05%) and quantifying FPV–Open separation at individual sampling dates using median abundances; ASVs were retained when peak FPV enrichment was supported across multiple dates and/or FPV ponds (Supplemental Methods).

Acknowledgements
This work was supported by an Atkinson Academic Venture Fund to SMG, MAH, MLS, awards 441993/2023-0 and 200781/2024-3 from National Council for Scientific and Technological Development (CNPq) to SJC, and startup funds from the University of Delaware made available to NER. We thank Benj Sterrett for helping to maintain access to the ponds, Autumn Newman, Augustus Pendleton, Sophia Richter and Kailyn Hanke for assistance with field and lab work, and Jera Jansen, Caitlin Davis, Mônica Antunes-Ulyssea, Sheena Dwyer-McNulty, Trifosa Simamora, Tim Boycott, and Dave Grodsky for helping construct the floating solar arrays.

References

Aben, R. C. H. and others. 2017. Cross continental increase in methane ebullition under climate change. Nat Commun 8: 1682. doi:10.1038/s41467-017-01535-y

Almeida, R. and others. 2022. Floating solar power: evaluate trade-offs. Nature 606: 246–249.

Andini, S., N. Suwartha, E. A. Setiawan, and S. Ma'arif. 2022. Analysis of biological, chemical, and physical parameters to evaluate the effect of floating solar PV in Mahoni Lake, Depok, Indonesia: Mesocosm experiment study. Journal of Ecological Engineering 23: 201–207. doi:10.12911/22998993/146385

Apprill, A., S. Mcnally, R. Parsons, and L. Weber. 2015. Minor revision to V4 region SSU rRNA 806R gene primer greatly increases detection of SAR11 bacterioplankton. Aquatic Microbial Ecology 75: 129–137. doi:10.3354/ame01753

Bastviken, D., J. Cole, M. Pace, and L. Tranvik. 2004. Methane emissions from lakes: Dependence of lake characteristics, two regional assessments, and a global estimate. Global Biogeochem Cycles 18: 1–12. doi:10.1029/2004GB002238

Bates, D., M. Maechler, B. Bolker, and S. Walker. 2015. Fitting linear mixed-effects models using lme4. J Stat Softw 67: 1–48. doi:10.1126/science.1176170

Bertolet, B. L., C. Koepfli, and S. E. Jones. 2022. Lake Sediment Methane Responses to Organic Matter are Related to Microbial Community Composition in Experimental Microcosms. Front Environ Sci 10. doi:10.3389/fenvs.2022.834829

Bertolet, B. L., West, W. E., Armitage, D. W., & Jones, S. E. 2019) Organic matter supply and bacterial community composition predict methanogenesis rates in temperate lake sediments. Limnol Oceanogr Lett, 4(5), 164-172.

Callahan, B. J., P. J. McMurdie, M. J. Rosen, A. W. Han, A. J. A. Johnson, and S. P. Holmes. 2016. DADA2: High-resolution sample inference from Illumina amplicon data. Nat Methods 13: 581–583. doi:10.1038/nmeth.3869

Caporaso, J. G., C. L. Lauber, W. A. Walters, D. Berg-Lyons, C. A. Lozupone, P. J. Turnbaugh, N. Fierer, and R. Knight. 2011. Global patterns of 16S rRNA diversity at a depth of millions of sequences per sample. Proc Natl Acad Sci U S A 108: 4516–4522. doi:10.1073/pnas.1000080107

Cazzaniga, R., and M. Rosa-Clot. 2021. The booming of floating PV. Solar Energy 219: 3–10. doi:10.1016/j.solener.2020.09.057

Dörenkämper, M., A. Wahed, A. Kumar, M. de Jong, J. Kroon, and T. Reindl. 2021. The cooling effect of floating PV in two different climate zones: A comparison of field test data from the Netherlands and Singapore. Solar Energy 219: 15–23. doi:10.1016/j.solener.2021.03.051

Gallaher, A., E. L. Kalies, and S. M. Grodsky. 2025. Sustainability trade-offs across modeled floating solar waterscapes of the Northeastern United States. Cell Reports Sustainability. doi:10.1016/j.crsus.2025.100423

Holgerson, M. A., Richardson, D. C., Roith, J., Bortolotti, L. E., Finlay, K., Hornbach, D. J., Gurung, K., Ness, A., Andersen, M. R., Bansal, S., Finlay, J. C., Cianci-Gaskill, J. A., Hahn, S., Janke, B. D., McDonald, C., Mesman, J. P., North, R. L., Roberts, C. O., Sweetman, J. N., & Webb, J. R. 2022. Classifying mixing regimes in ponds and shallow lakes. Water Resour Res, 58(7), e2022WR032522.

Ilgen, K., D. Schindler, S. Wieland, and J. Lange. 2023. The impact of floating photovoltaic power plants on lake water temperature and stratification. Sci Rep 13. doi:10.1038/s41598-023-34751-2

Jackson, R. B. and others. 2024. Human activities now fuel two-thirds of global methane emissions. Environmental Research Letters 19: 101002. doi:10.1088/1748-9326/ad6463

Jin, Y. and others. 2023. Energy production and water savings from floating solar photovoltaics on global reservoirs. Nat Sustain 6: 865–874. doi:10.1038/s41893-023-01089-6

Knief, C. 2015. Diversity and habitat preferences of cultivated and uncultivated aerobic methanotrophic bacteria evaluated based on pmoA as molecular marker. Frontiers in Microbiology 6: 1346.

Lenth, R. 2018. emmeans: Estimated marginal means, aka least-squares means. R package version 1.2.3.

Li, B., Z. Mao, J. Xue, P. Xing, and Q. L. Wu. 2024. Metabolic versatility of aerobic methane-oxidizing bacteria under anoxia in aquatic ecosystems. Environmental Microbiology Reports 16. doi:10.1111/1758-2229.70002

Lin, H., and S. Das Peddada. 2024. Multigroup analysis of compositions of microbiomes with covariate adjustments and repeated measures. Nat Methods 21: 83–91. doi:10.1038/s41592-023-02092-7

Louca, S., L. Parfrey, and M. Doebeli. 2016. Decoupling function and taxonomy in the global ocean microbiome. Science 353: 1272–1277. doi:10.1126/science.aad8279

Lyautey, E., Billard, E., Tissot, N., Jacquet, S., & Domaizon, I. 2021. Seasonal dynamics of abundance, structure, and diversity of methanogens and methanotrophs in lake sediments. Microb Ecol, 82(3), 559-571.

McDonald, D. and others. 2024. Greengenes2 unifies microbial data in a single reference tree. Nat Biotechnol 42: 715–718. doi:10.1038/s41587-023-01845-1

McMurdie, P. J., and S. Holmes. 2013. Phyloseq: An R Package for Reproducible Interactive Analysis and Graphics of Microbiome Census Data. PLoS One 8: e61217. doi:10.1371/journal.pone.0061217

Milucka, J., Kirf, M., Lu, L., Krupke, A., Lam, P., Littmann, S., Kupers, M. M. M., and Schubert, C. J. 2015. Methane oxidation coupled to oxygenic photosynthesis in anoxic waters. ISME J 9(9), 1991-2002.

Murase, J., & Sugimoto, A. 2005. Inhibitory effect of light on methane oxidation in the pelagic water column of a mesotrophic lake (Lake Biwa, Japan). Limnol Oceanogr, 50, 1339-1343.

Nobre, R., S. M. Rocha, S. Healing, Q. Ji, S. Boulêtreau, A. Armstrong, and J. Cucherousset. 2024. A global study of freshwater coverage by floating photovoltaics. Solar Energy 267. doi:10.1016/j.solener.2023.112244

Oksanen, J. and others. 2018. vegan: Community Ecology Package. R package version 2.5.

Parada, A. E., D. M. Needham, and J. A. Fuhrman. 2016. Every base matters: Assessing small subunit rRNA primers for marine microbiomes with mock communities, time series and global field samples. Environ Microbiol 18: 1403–1414. doi:10.1111/1462-2920.13023

R Core Team. 2014. R: A language and environment for statistical computing.

Ramanan, C. J., K. H. Lim, J. C. Kurnia, S. Roy, B. J. Bora, and B. J. Medhi. 2024. Towards sustainable power generation: Recent advancements in floating photovoltaic technologies. Renewable and Sustainable Energy Reviews 194: 114322. doi:10.1016/j.rser.2024.114322

Ray, N. E., and M. A. Holgerson. 2023. High intra-seasonal variability in greenhouse gas emissions from temperate constructed ponds. Geophys Res Lett 50: e2023GL104235. doi:10.1029/2023GL104235

Ray, N. E., M. A. Holgerson, and S. M. Grodsky. 2024. Immediate Effect of floating solar energy deployment on greenhouse gas dynamics in ponds. Environ Sci Technol 58: 22104–22113. doi:10.1021/acs.est.4c06363

Reis, P. C. J. and others. 2020. Niche separation within aerobic methanotrophic bacteria across lakes and its link to methane oxidation rates. Environ Microbiol 22: 738–751.

Reis, P. C. J. and others. 2024. Enigmatic persistence of aerobic methanotrophs in oxygen-limiting freshwater habitats. ISME J 18: wrae041.

Rissanen, A. J., Saarela, T., Jäntti, H., Buck, M., Peura, S., Aalto, S. L., Ojala, A., Pumpanen, J., Tirola, M., Elvert, M., and Nykänen, H. 2021. Vertical stratification patterns of methanotrophs and their genetic controllers in water columns of oxygen-stratified boreal lakes. FEMS Microb Ecol, 97(2), fiaa252.

Thottathil, S. D., Reis, P. C., del Giorgio, P. A., & Prairie, Y. T. 2018. The extent and regulation of summer methane oxidation in northern lakes. J Geophys Res: Biogeosci, 123(10), 3216-3230.

van Grinsven, S., Sinninghe Damsté, J. S., Abdala Asbun, A., Engelmann, J. C., Harrison, J., & Villanueva, L. 2020. Methane oxidation in anoxic lake water stimulated by nitrate and sulfate addition. Environ Microbiol, 22(2), 766-782.

Wang, B., E. Stirling, Z. He, B. Ma, H. Zhang, X. Zheng, F. Xiao, and Q. Yan. 2021. Pollution alters methanogenic and methanotrophic communities and increases dissolved methane in small ponds. Science Tot Environ 801. doi:10.1016/j.scitotenv.2021.149723

Wang, T. W. and others. 2022. Effects of floating photovoltaic systems on water quality of aquaculture ponds. Aquac Res 53: 1304–1315. doi:10.1111/are.15665

Wickham, H. 2016. ggplot2: Elegant Graphics for Data Analysis, Springer-Verlag.

Woolway, R. I., G. Zhao, S. M. G. Rocha, S. J. Thackeray, and A. Armstrong. 2024. Decarbonization potential of floating solar photovoltaics on lakes worldwide. Nature Water 2: 566–576. doi:10.1038/s44221-024-00251-4